

HOW BEACH STATE INFLUENCES WAVE RUNUP ON A PERCHED BEACH IN SOUTHWESTERN AUSTRALIA

Carly Portch, The University of Western Australia, carly.portch@research.uwa.edu.au

Michael Cuttler, The University of Western Australia, michael.cuttler@uwa.edu.au

Mark Buckley, U.S. Geological Survey, mbuckley@usgs.gov

Jeff Hansen, The University of Western Australia, jeff.hansen@uwa.edu.au

Ryan Lowe, The University of Western Australia, ryan.lowe@uwa.edu.au

INTRODUCTION

Approximately 20 to 30% of the world's coastlines are fronted by shallowly buried or outcropping shore platforms overlain by perched beaches (Kirk, 1977; Marshall & Stephenson, 2011; Trenhaile, 2002). Seasonal erosion of perched sediment can shift the beach state from 'accreted' to 'exposed' (Gallop et al., 2011), and the effect this has on wave-induced flood risk (known as wave runup) is unknown. As sea levels rise and storm severity increases, understanding how beach state influences wave runup is crucial for minimising coastal hazard risk and managing perched beach coastlines.

Runup is comprised of a time-averaged (setup, η), and time-varying (swash, $S_{2\%}$) component. Setup is primarily generated from wave breaking (which can be prevalent seaward of and on the edge of shore platforms). The remaining waves that reach the shoreline generate oscillations known as swash (Miche, 1951), which in combination with setup produces total runup. On perched beaches, the underlying shore platform has been found to reduce wave heights by 33%, and dissipate wave energy to less than 7% the energy seaward of the platform (Moura et al., 2012; Stephenson & Kirk, 2000). How these nearshore processes translate to the shoreline in the form of runup has not yet been investigated.

In this work, idealised numerical modelling and field observations along a perched beach in southwestern Australia were used to quantify the influence of beach state on wave runup, setup, and swash processes.

METHODS

An 8-month field campaign was conducted along a perched beach in Albany, Western Australia with large erosion/accretion cycles and significant offshore wave heights (H_o) ranging from 1 - 8 m. A stationary georeferenced camera system (Holman & Stanley, 2007), 3 nearshore pressure sensors, an offshore wave buoy, and monthly drone surveys were used to quantify wave runup at seven cross-shore transects across a range of wave conditions, tidal levels, and beach states.

The Structure-from-Motion technique (Seymour et al., 2017; Snavely et al., 2008; Turner et al., 2016; Warrick et al., 2017) was applied to drone images to obtain monthly beach topography, and a ground-based RTK-GPS survey was used to obtain the slope and elevation of the underlying platform. The beach was classified as 'exposed' when the shore platform was visible, and 'accreted' when it was not visible. The instantaneous shoreline positions were digitised from the geo-rectified

imagery at each cross-shore location over a 25-minute time interval. An idealised linear profile was generated to represent the complex nearshore topo-bathymetry. This was done by finding the linear slope, β_i , that minimises the standard deviation between the actual profile and the idealised profile. The shoreline observations were projected onto this idealised profile to obtain a vertical elevation time series. This time series was used to calculate extreme runup ($R_{2\%}$), setup (η), and swash ($S_{2\%}$) statistics for 100 individual cases across 'exposed' and 'accreted' beach states using well-documented techniques (Stockdon et al., 2006).

A complimentary numerical modelling study was conducted using SWASH to compare the nearshore hydrodynamic response of an 'exposed' shore platform to an 'accreted' shore platform (analogous to a plane sloping beach). The SWASH model was run in a two-dimensional vertical (2DV) plane, with 1 m grid resolution and 2 vertical layers. It was validated against two existing physical model tests of a sandy sloping foreshore with a shallow dike (Streicher et al., 2017; Suzuki et al., 2017).

Both the 'accreted' and 'exposed' profiles had a slope of 1:30 from 15 m depth to 5 m above the still water level (SWL). The 'exposed' profile had a 50 m wide horizontal shore platform outcropping at 0 m depth, with a seaward edge slope of 1:2. The offshore SWASH boundary was forced with a JONSWAP spectrum with a significant wave height of 2 m, and a peak wave period of 10 s. The SWL was set to 0.5 m above the horizontal shore platform.

The instantaneous shoreline position was defined as the most seaward cross-shore grid cell with a water depth equal to or below 5 cm (minimum depth threshold). This was calculated at every time step to produce a shoreline time series, which was used to calculate runup statistics from the same techniques used for field observations. Instantaneous water levels and velocities were output at 5 m increments across the cross-shore profile to analyse the nearshore hydrodynamic processes. A frequency domain algorithm (assuming linear wave theory) (Buckley et al., 2015) was used to perform a directional wave analysis to separate the incoming and outgoing waves. The incoming and outgoing water levels and velocities that were produced were used to calculate incoming and outgoing significant wave heights and the reflection coefficient (R_c) at each cross-shore position.

RESULTS AND DISCUSSION

From field observations, runup for both 'accreted' and 'exposed' beach states were found to scale similarly with the parameter incorporating offshore wave conditions and

idealised beach slope, $\beta_i(H_oL_o)^{1/2}$ (Figure 1a). For a given $\beta_i(H_oL_o)^{1/2}$ value, setup was often larger for the 'exposed' cases compared to the 'accreted' cases (Figure 1b), and swash was larger for the 'accreted' cases compared to the 'exposed' cases (Figure 1c). For example, for a $\beta_i(H_oL_o)^{1/2}$ value of 0.22 m, setup is up to 1 m larger for the 'exposed' beach state, and swash is up to 1.5 m larger for the 'accreted' beach state.

This results in primarily setup-dominated runup when in an 'exposed' beach state, and primarily swash-dominated runup when in an 'accreted' beach state (Figure 1b,c). This trends across the entire range of beach slopes and wave conditions in the dataset.

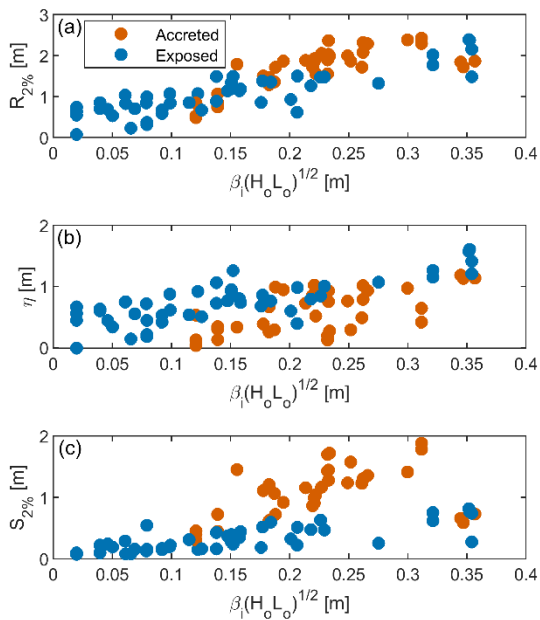


Figure 1 - (a) The parameter, $\beta_i(H_oL_o)^{1/2}$, plotted against (a) runup ($R_{2\%}$), (b) setup (η), and (c) swash ($S_{2\%}$) measured at the Torbay field site during both 'accreted' (orange marker) and 'exposed' (blue marker) beach states.

The significant variability in setup and swash contributions suggest that different hydrodynamic processes were driving runup during different beach states. This may be caused by variability in beach slope, bottom roughness, shore platform exposure, or a variety of other morphological factors that are influenced by change in beach state.

To investigate the impact of the exposure of the shore platform edge, complimentary SWASH simulations were conducted. The nearshore hydrodynamics of a plane beach (analogous to an 'accreted' beach state where the shore platform is not visible), were compared to an identical plane beach with an outcropping shore platform (analogous to an 'exposed' beach state where the shore platform is visible) (Figure 2).

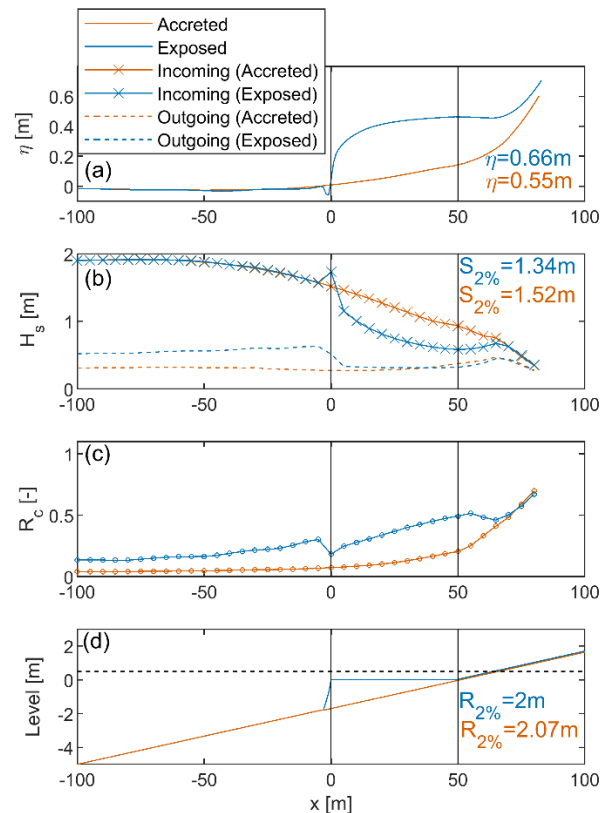


Figure 2 - A comparison of simulated nearshore bulk parameters for an idealised 'accreted' (orange) and 'exposed' (blue) beach state using SWASH. An offshore wave height (H_o) of 2 m, and peak period (T_p) of 10 s were forced at the offshore boundary in 15 m water depth. All bulk parameters are presented at 5 m intervals across the cross-shore profile until the mean shoreline position is reached. The (a) setup (η), (b) significant incoming (x marker) and outgoing (-marker) wave heights (H_s), and (c) reflection coefficients (R_c) are presented for the 'accreted' and 'exposed' transects. (d) The 'accreted' and 'exposed' beach profiles are displayed with the default still water level (SWL) indicated by the horizontal dashed line. The seaward (left) and shoreward (right) edges of the platform are indicated in all panels by the vertical solid lines. The setup (η), swash ($S_{2\%}$), and runup ($R_{2\%}$) values measured at the shoreline are presented in panel (a), (b), and (d), respectively.

Concentrated wave breaking at the shore platform edge resulted in an increase in setup across the platform (Figure 2a), which resulted in a 0.11 m increase in setup at the shoreline compared to an 'accreted' beach state. The significant wave heights were reduced at the shore platform edge due to wave breaking and partial wave reflection (Figure 2b). The reflection coefficient (R_c) increased as waves propagated towards the shore platform ($x < 0$ m), then decreased slightly once waves overtopped the shore platform ($x > 0$ m), suggesting partial wave reflection at the shore platform edge (Figure 2c). There was also a ~ 0.2 m increase in outgoing wave heights at the shore platform edge due to the superposition of outgoing reflected waves from the shoreline and outgoing reflected waves from the platform edge (Figure 2b). This led to an overall reduction in swash

energy at the shoreline by 0.18 m compared to the 'accreted' case.

Despite the significant difference in nearshore hydrodynamics on an 'accreted' and 'exposed' profile, there was a small 0.07 m difference between overall runup on the idealised 'accreted' and 'exposed' beach profiles (Figure 2d), due to the opposing effects of the shore platform edge on setup and swash. This aligns with the field observations in Albany, Western Australia, where runup for both beach states was primarily driven by offshore wave conditions and beach slope, yet the 'exposed' beach state was predominantly setup-dominated, while the 'accreted' beach state was predominantly swash-dominated.

These results have implications for improving runup predictions and coastal management on perched beaches with significant sediment transport and seasonal variability. It highlights the importance of accounting for beach state change when assessing coastal hazards along perched beaches.

REFERENCES

- Buckley, Lowe, Hansen, Van Dongeren (2015): Dynamics of wave setup over a steeply sloping fringing reef, *Journal of Physical Oceanography*, vol 45, pp. 3005-3023.
- Gallop, Bosserelle, Pattiaratchi, Eliot (2011): Rock topography causes spatial variation in the wave, current and beach response to sea breeze activity, *Marine Geology*, vol 290, pp. 29-40.
- Holman, Stanley (2007): The history and technical capabilities of Argus, *Coastal Engineering*, vol 54, pp. 477-491.
- Kirk (1977): Rates and forms of erosion on intertidal platforms at Kaikoura Peninsula, South Island, New Zealand, *New Zealand Journal of Geology and Geophysics*, vol 20, pp. 571-613.
- Marshall, Stephenson (2011): The morphodynamics of shore platforms in a micro-tidal setting: Interactions between waves and morphology, *Marine Geology*, vol 288, pp. 18-31.
- Miche (1951): Le pouvoir réfléchissant des ouvrages maritimes, *Ann Ponts, Chausees*, vol 121, pp. 285-319.
- Moura, Gabriel, Gamito, Tavares, Martins (2012): Integrated assessment of bioerosion, biocover and downwearing rates of carbonate rock shore platforms in southern Portugal, *Continental Shelf Research*, vol 38, pp. 79-88.
- Seymour, Ridge, Rodriguez, Newton, Dale, Johnston (2017): Deploying Fixed Wing Unoccupied Aerial Systems (UAS) for Coastal Morphology Assessment and Management, *Journal of Coastal Research*, vol 34, pp. 704-717.
- Snavely, Seitz, Szeliski (2008): Modeling the world from Internet phone collections, *International Journal of Computer Vision*, vol 80, pp. 189-210.
- Stephenson, Kirk (2000): Development of shore platforms on Kaikoura Peninsula, South Island, New Zealand II: The role of subaerial weathering, *Geomorphology*, vol 32, pp. 43-56.
- Stockdon, Holman, Howd, Sallenger (2006): Empirical parameterization of setup, swash, and runup, *Coastal Engineering*, vol 53, pp. 573-588.
- Streicher, Kortenhaus, Altomare, Gruwez, Hofland, Chen, Marinov, Scheres, Schüttrumpf, Hirt (2017): WALOWA (WAVE LOADS ON WALLS): Large-Scale Experiments in the Delta Flume, *International Short Course and Conference on Applied Coastal Research (SCACR)*, pp. 69-80.
- Suzuki, Altomare, Veale, Verwaest, Trouw, Troch, Zijlema (2017): Efficient and robust wave overtopping estimation for impermeable coastal structures in shallow foreshores using SWASH, *Coastal Engineering*, vol 122, pp. 108-123.
- Trenhaile (2002): Rock coasts, with particular emphasis on shore platforms, *Geomorphology*, vol 48, pp. 7-22.
- Turner, Harley, Drummond (2016): UAVs for coastal surveying, *Coastal Engineering*, vol 114, pp. 19-24.
- Warrick, Ritchie, Adelman G, Adelman K, Limber (2017): New Techniques to Measure Cliff Change from Historical Oblique Aerial Photographs and Structure-from-Motion Photogrammetry, *Journal of Coastal Research*, vol 331, pp. 39-55.